Research Article | Vol. 33, No. 8 / 21 Apr 2025 / Optics Express 17551
Optics EXPRESS

Spatio-temporal diagnosis of few-cycle 3.2 µm pulses from a mid-IR OPCPA system

ROLAND S. NAGYMIHÁLY,[1,*] BÁLINT KISS,[1] MIGUEL MIRANDA,[2] MATIAS CHARRUT,[2] PAULO T. GUERREIRO,[2] LEVENTE LEHOTAI,[1] RAJARAM SHRESTHA,[1] ERIC CORMIER,[1,3] AND ROSA ROMERO[2]

[1]*ELI ALPS Research Institute, Wolfgang Sandner u. 3, 6728-Szeged, Hungary*
[2]*Sphere Ultrafast Photonics, Rua do Campo Alegre, n.° 1021, Edifício FC6 4169-007 Porto, Portugal*
[3]*Laboratoire Photonique Numérique et Nanosciences (LP2N), UMR 5298, CNRS-IOGS-Université Bordeaux, 33400 Talence, France*
[*]*roland.nagymihaly@eli-alps.hu*

Abstract: Four-cycle pulses from a 3.2 µm OPCPA system were characterized by spatially resolved Fourier transform spectroscopy, for the first time. Combining the spatio-spectral information with temporal characterization yielded the spatio-temporal structure of the pulses revealing up to now inaccessible details in the mid-IR spectral region. The proposed technique offers efficient and simple characterization for the optimization of MIR OPCPA systems in terms of spatio-spectral couplings.

1. Introduction

Mid-infrared (MIR) ultrashort pulses are key tools for ultrafast spectroscopy [1], strong-field phenomena [2], and lately they have been extensively used to generate high harmonics from different solids [3], as well. High harmonic generation with few-to-single-cycle laser pulses is known to be as a highly phase sensitive phenomenon [4]. Laser pulses of such sources must exhibit very large spectral bandwidth, which makes them sensitive to spatio-spectral, and consequently, to spatio-temporal couplings (STCs) [5]. Such distortions can originate from different parts of the laser system and are detrimental to achieving the required intensity in nonlinear light-matter interaction experiments. MIR few-cycle pulses in the spectral range of 1.5–4 µm are typically obtained from optical parametric chirped pulse amplification (OPCPA) systems pumped by Yb-based sub-ps lasers centered around 1 µm wavelength [6–9]. Because of the conservation laws intrinsic to these parametric processes, spatio-temporal couplings may easily emerge if particular attention is not paid in the implementation, thus requiring a proper accurate diagnostic.

Spatial diagnosis of MIR pulses can be performed with cameras based on pyroelectric and microbolometer technology, or alternatively with expensive CCD sensors based on InSb. These provide only spectrally integrated information about the intensity distribution in the transversal cross-section of the beam. The spectral content of MIR pulses is accessible by using optical spectrum analyzers, spectrographs or even spectrometers based on acousto-optic programmable dispersive filters (AOPDF like MOZZA, Fastlite). However, unless 2D spectrometers are used, the spectra are spatially integrated. In the recent years, several techniques have been proposed and adapted to perform a temporal reconstruction of MIR laser pulses beyond 2 µm, like for instance frequency resolved optical gating [10], dispersion scan [11], or the TIPTOE [12] technique to cite a few. Note that these methods provide the temporal characteristics averaged over the entire (or partial) extension of the beam. In the near infrared spectral region several methods (TERMITES [13], ICE [14]) have been proposed to perform complete spatio-spectral reconstruction of laser pulses based on spatially resolved Fourier transform spectroscopy with different interferometric implementations. Furthermore, spatially resolved Fourier transform spectroscopy combined with

#561914 https://doi.org/10.1364/OE.561914
Journal © 2025 Received 13 Mar 2025; accepted 19 Mar 2025; published 11 Apr 2025

Optics EXPRESS

an iterative phase retrieval algorithm, called INSIGHT [15], was proven to be also a very effective tool to provide spatio-spectral diagnosis on near-IR pulses [16]. These techniques perform the actual measurement in either the near or the far field, but with the use of advanced propagation algorithms they can provide spatial information in practically any plane at any frequency about the measured pulse. If the spatio-spectral measurement is combined with a temporal characterization of the same pulse at any spatial point of the beam cross-section, the complete spatio-temporal map of the pulse can be reconstructed.

New implementations of TERMITES combined the spatio-spectral reconstruction with frequency resolved optical gating, through which post-compressed 800 nm pulses were characterized in the spatio-temporal domain [17]. Further development of this technique resolved also the phase structure of vortex beams in the NIR spectral region [18]. Similar vortex pulses were measured by using the nano-TIPTOE technique, where a nanometric needle tip is placed in the focus [19].

Recently, spatio-temporal measurements were conducted by using imaging based on electro-optic sampling in the NIR to MIR region in case of light transients [20]. Furthermore, the TIPTOE technique was also implemented with spatial resolution by using a camera-based detection system and tested with a 3 μm few-cycle radially polarized vector beam [21].

Direct measurements with TERMITES or INSIGHT type of methods were never conducted in the MIR spectral range, to the best of our knowledge, mainly due to availability of suitable detectors with proper spatial resolution and spectral sensitivity. Spatial intensity distribution at different wavelengths was only recently investigated by using the Fourier transform imaging spectrometer technique in the context of a MIR OPA. However, the spectral phase was not retrieved [22]. The detection was performed using a 2D microbolometer array.

Here we present the implementation of the ICE technique with MIR laser pulses, for the first time. To accomplish this, we used an interferometer with metal coated optics, after which the recombined beams are sent to a high-resolution MIR CCD camera. Spatio-temporal reconstruction is facilitated by combining the ICE results with temporal characterization by using the TIPTOE technique.

2. Experimental scheme

Our experiment used the MIR OPCPA system of the ELI ALPS Facility (BLACK STARZZ, Fastlite [6]), which currently emits 45 fs full width at half maximum (FWHM) pulses centered at 3.2 μm wavelength with 100 kHz repetition rate and 10 W of average power [23]. The OPCPA is pumped by an Yb:YAG thin disk regenerative amplifier (Dira200-100, TRUMPF Scientific Lasers) with 1.1 ps pulses of currently 175 W average power at 100 kHz. Out of 175 W, a portion of 25 W is post-compressed to 100 fs while the remaining 150 W is used to pump the MIR OPCPA. A small portion of the pump beam is used to generate a supercontinuum, which is phase and amplitude-shaped by a DAZZLER. The supercontinuum is then mixed with the pump pulses in a self-seeded difference frequency generation stage (1 mm MgO:PPLN, collinear), producing a broadband and passively phase-stable seed at 3200 nm central wavelength. The 3200 nm seed is then amplified further in one collinear OPA stage (0.7 mm MgO:PPLN) and two non-collinear OPA stages (1.5 mm bulk undoped Lithium Niobate). The amplified pulses are compressed in 20 mm thick bulk silicon and 1 mm sapphire (output window) with a final output of 100 μJ and 45 fs pulse duration. Further details on the OPCPA can be found in Ref. [6].

In order to have a glimpse into the spatio-spectral and spatio-temporal structure of MIR laser pulses, we realized an experimental setup with two wire grid polarizers (variable attenuator), and an all reflective down-collimating telescope to fit the input energy and beam size requirements of all diagnostic devices (Fig. 1(a)). The polarizers were slightly tilted with opposite directions to mitigate back-reflections and spatial walk-off. High-resolution spectral measurement was performed by an AOPDF-based spectrometer (MOZZA, Fastlite) with a dynamic range above 30

Optics EXPRESS

dB. For temporal characterization, we used the TIPTOE technique (SourceLab), which is based on ionization in ambient air [12].

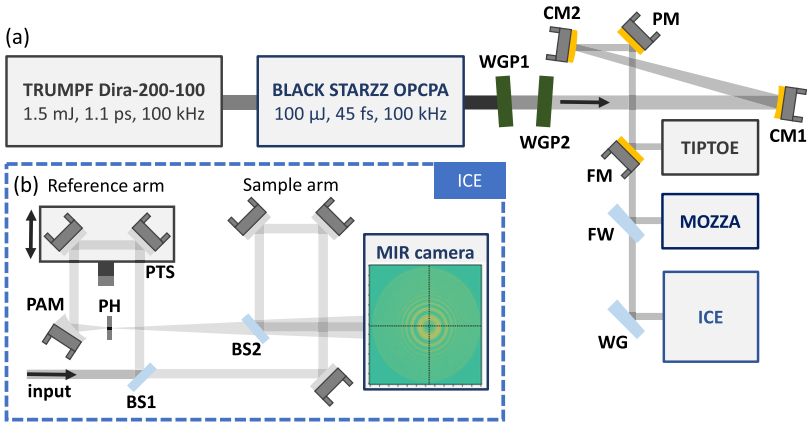

Fig. 1. Schematic layout of the experimental setup (a). WGP1 and WGP2 are wire grid polarizers, CM1 is a concave and CM2 is a convex spherical mirror, PM is a plane mirror, FM is a flip mirror, FW is a flip CaF2 wedge, while WG is a CaF2 wedge. Schematic picture of the ICE arrangement is shown in (b). BS1 and BS2 are beamsplitters, PTS is a piezo linear translation stage, PAM is a parabolic mirror and PH is a pinhole.

The spatio-spectral characterization of the MIR pulses is achieved by implementing the integral characterization engine (ICE) technique [14], which is based on spatially resolved Fourier transform spectroscopy (Fig. 1(b)). The pulses to be characterized are coupled into a Mach-Zehnder interferometer. In the reference arm after BS1, the beam is focused by a 50 mm focal length parabolic mirror into a pinhole with 50 µm diameter at the focus. The pinhole acts like an ideal point source, which creates a spherical wave with high-quality wavefront. In the sample arm, an appropriate temporal delay is created to match that of the reference arm, without any modification in the beam. The two beams are recombined by a second beamsplitter (Fig. 1(b), BS2). A piezo driven linear translation stage (Fig, 1, b, PTS) with a total travel range of 150 µm was used to cover a temporal scanning range of 1024 fs with a minimal temporal step size of 0.25 fs. Spectral resolution accounts for 33.4 nm at 3200 nm, accordingly. The output of the interferometer is coupled to a MIR CCD camera (IRC912, IRCameras). Every pixel of the CCD therefore measures the linear cross-correlation between the reference and sample pulses for different temporal delays, which results in a spatially resolved temporal measurement. The measured cross-correlation signal is analyzed then in the frequency domain after applying Fourier transform on it. Taken the homogeneous reference pulse originating from the spatially filtered reference arm, the spectral amplitude and phase of the input pulse can be determined at any spatial coordinate [14]. The MIR camera was selected in accordance with the spatial resolution requirements for the ICE technique: it provides a resolution of 1280×1024 pixels with pixel size of 12 µm, and an effective sensitivity of the chip between 900 and 5500 nm. We performed multiple measurements with ICE with different step sizes and temporal scan ranges, from which we present here the one with the highest spectral resolution. Nevertheless, reproducibility of the measurements was found to be very good, with almost identical results.

3. Spectral and temporal characterization

The OPCPA output beam was first coupled to the MOZZA spectrometer, which can provide a high-resolution and high-dynamic spectral intensity distribution measurement (without spatial information). Front surface reflection from a CaF_2 wedge was used to attenuate further the beam

Optics EXPRESS

after the wire grid polarizers. A typical spectrum measured after the wire grid polarizers is shown in Fig. 2(a).

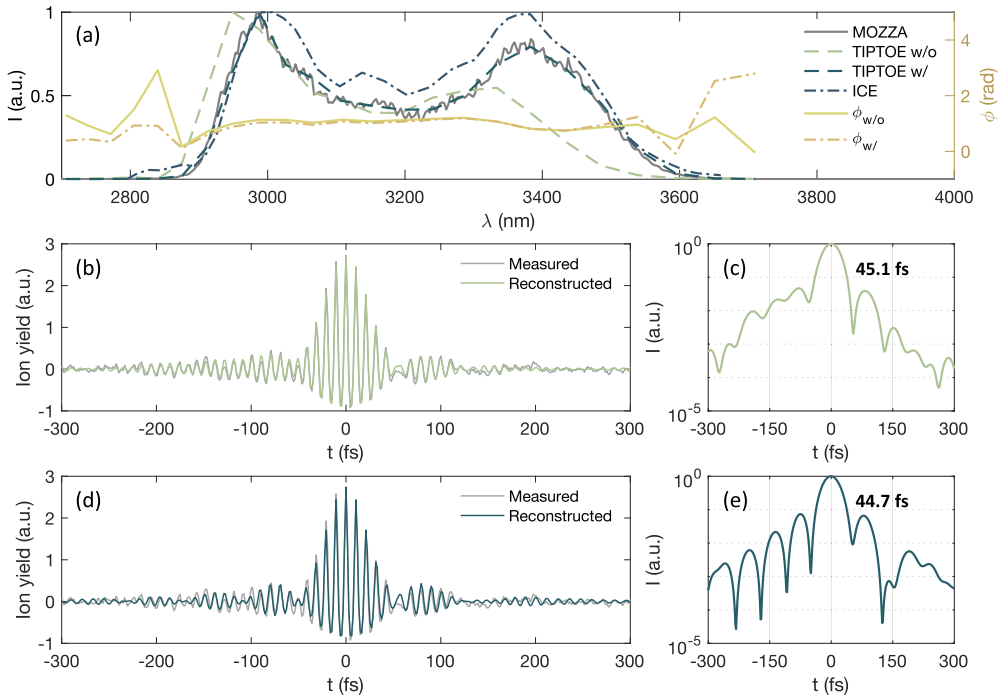

Fig. 2. OPCPA spectrum measured by different techniques (a): MOZZA in sub-aperture (grey line), TIPTOE reconstruction without and with externally measured spectrum (green and blue dashed line) and ICE on axis (dark blue dashed), TIPTOE reconstructed phase without and with externally measured spectrum (green continuous orange dashed). Normalized ion yield of TIPTOE from the measurement (grey) and reconstruction (green and blue) without (b) and with externally measured spectrum (d). Respective temporal intensity profiles from TIPTOE (c and e), where FWHM pulse duration values are also highlighted.

As the temporal characterization requires to ionize ambient air, the energy is adjusted by rotating the wire grids to reach 40 µJ pulse energy at the input of the TIPTOE device. It was previously confirmed, that tuning the wire grid polarizers does not change the spectrum or the compression of the transmitted pulses. Reconstruction of the TIPTOE measurement without and with the incorporated MOZZA spectrum gave high quality 45.1 and 44.7 fs pulses (Fig. 2), respectively, and an FTL duration of 44 fs. It is necessary to further attenuate the pulse energy for the ICE arrangement, thus the front surface reflection of a CaF_2 wedge is used after the polarizers, again.

4. Spatio-spectral characterization

In practice, ICE retrieves both the amplitude and the phase across the beam for any wavelength in the spectrum. Consequently, the spatial intensity profile and the phase is spectrally resolved. As an example, the complex spatial field is displayed for 6 different wavelengths in Fig. 3. Input aperture of the MIR camera limited the usable beam size to about 11 mm. The intensity profiles in Fig. 3 are normalized to the maximal spectral intensity. The spectral phase shows a small distortion around the left edge of the beam from 3000 up to 3400 nm in the horizontal

Optics EXPRESS

cross-section, while the intensity profile does not show any significant changes by scanning the wavelength and remains Gaussian in distribution.

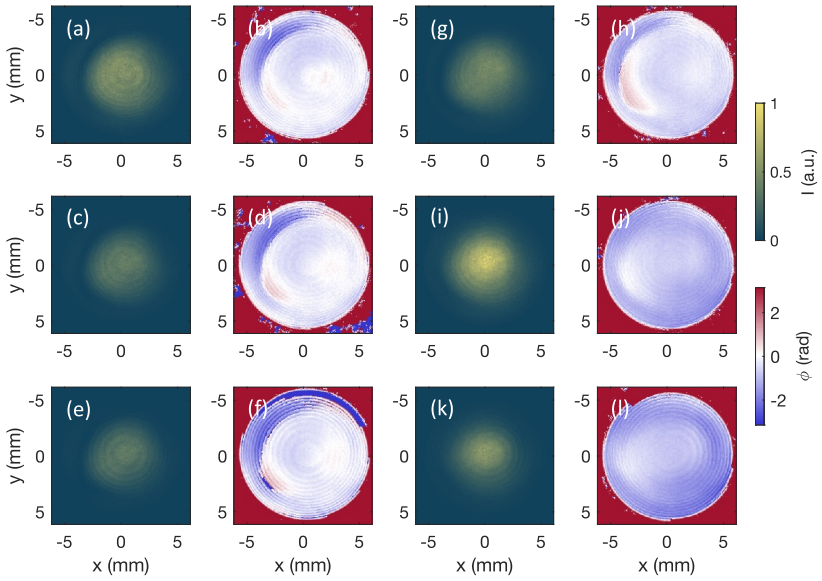

Fig. 3. Spatial profile and phase from the ICE retrieval at the following wavelengths: 3014 nm (a, b), 3105 nm (c, d), 3203 nm (e, f), 3306 nm (g, h), 3416 nm (i, j), 3494 nm (k, l).

Results on the spatio-spectral intensity distribution in the near field show highly homogeneous spectral content of the MIR pulses. However, while in the horizontal direction there is only a negligible amount of 0.6 µm/nm spatial chirp, in the vertical direction a noticeable tilt of -14 µm/nm has been identified (Fig. 4(a) and (c)).

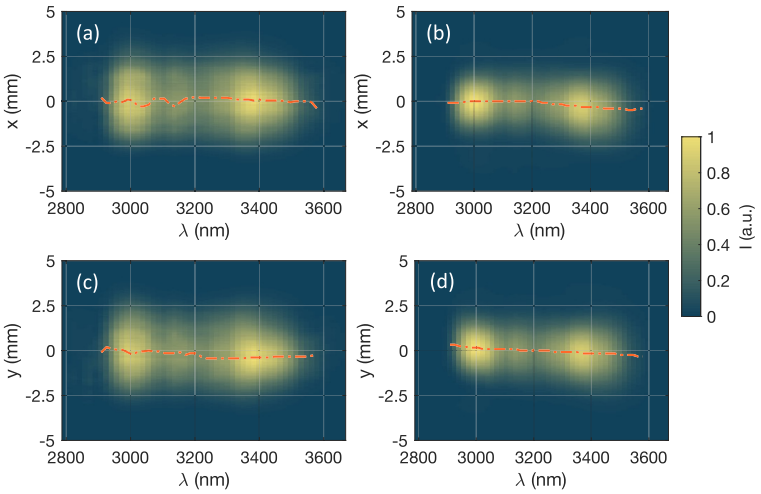

Fig. 4. Spatially resolved spectra retrieved from the ICE measurement: horizontal (a) and vertical (c) cross-sections in the near field, horizontal (b) and vertical (d) cross-sections in the far field. Orange dashed curves represent the intensity maxima at different wavelengths.

Optics EXPRESS

In the far field, the quality is similar. We see a residual angular dispersion of -9.5 µrad/nm in the output pulses of the OPCPA in the horizontal cross-section (Fig. 4(b)). In the other direction, the vertical cross-section also shows a small tilt of -10 µrad/nm (Fig. 4(d)). The residual angular dispersion in the horizontal direction is attributed to the noncollinear phase matching in the OPA stages. On the other hand, the vertical angular dispersion is most probably due to a slight pulse front tilt imprinted from the pump beam. The spectral shape reconstruction from ICE shows very good agreement with the direct spectrometer measurement, as well (Fig. 2(a)). It was already shown that the spectral phase of parametrically amplified pulses can exhibit distortions in the transverse cross-sections of the beam [16]. For this reason, the structure of the spectral phase was analyzed along the central transverse cross-sections of the MIR pulses (Fig. 5(a) and (b)). We only found noticeable distortion in the phase structure around -4 mm position, which spans from 2900 nm up to 3400 nm in the spectrum (Fig. 5(a)).

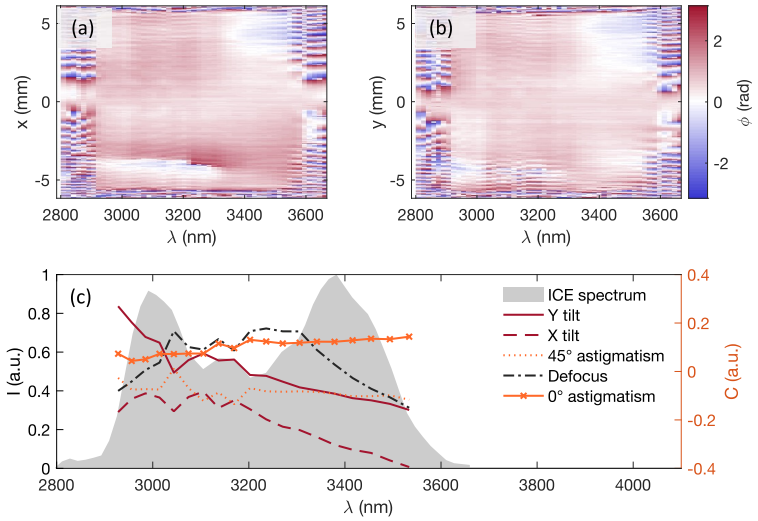

Fig. 5. Spectrally resolved phase distribution in the central cross-section of the OPCPA beam in the x and y directions (a and b). Reconstructed spectrum in the center of the beam with the spectrally dependent Zernike polynomial coefficients of the first few orders (c).

The origin of this phase deformation is currently unknown, but it appears at the low intensity edge of the beam, thus we think it has a negligible effect on the compressed pulses. Zernike polynomial decomposition of the spectrally dependent wavefront yields negligible chromatic aberrations up to an order of 10 (Fig. 5(c)). Figure 5(c) shows only the first few Zernike coefficients, which are typically contributing to wavefront distortions in amplified beams, but higher orders are becoming less and less significant along the complete laser spectrum. Tilts in horizontal and vertical directions are corresponding to the observed angular dispersion from Fig. 4. Spectral dependence of the defocus is practically insignificant, being a second order effect, similar coefficient values as tilts will not lead to noticeable deformations on the pulse. Furthermore, based on Fig. 5, either of the astigmatism coefficients is showing significant spectral variation.

5. Spatio-temporal reconstruction

By utilizing the spectral phase retrieved by the TIPTOE technique with an independently measured spectrum from the MOZZA, we could fully reconstruct the spatio-temporal intensity profile of the OPCPA pulses in the horizontal and vertical cross-sections. Here we note, that in the TIPTOE measurement, most of the beam contributes to the electron yield measured by the electrodes.

Optics EXPRESS

Consequently, a spatially averaged temporal duration is measured. The average spectral phase derived from the temporal shape of the measured electric field is used as a reference for the ICE post-processing. We believe that this is a good approximation in terms of reference spectral phase for the complete spatio-temporal reconstruction, because the measured pulses had only minor spatio-spectral couplings. As it can be deduced from Fig. 2, the compression of the pulses was close to ideal.

Consequently, the retrieved spectral phase has minor effects in the spatio-temporal intensity distribution of the compressed pulses, which is visualized in Fig. 6 for both cross-sections. Slight intensity modulations along the spatial axis are caused by measurement noise. In Fig. 6(c and d), one can observe, that the pulse exhibits very minor pulse front tilt in both the horizontal and vertical cross-sections, as a consequence of the residual angular dispersion. At the same time, the phase front is practically flat for both directions. A more accurate way to perform the reference temporal characterization would be to either measure a small central part of the beam, or to measure the spatially filtered reference beam. However, since TIPTOE requires significant amount of the available pulse energy, in our experiment this was not possible to accomplish.

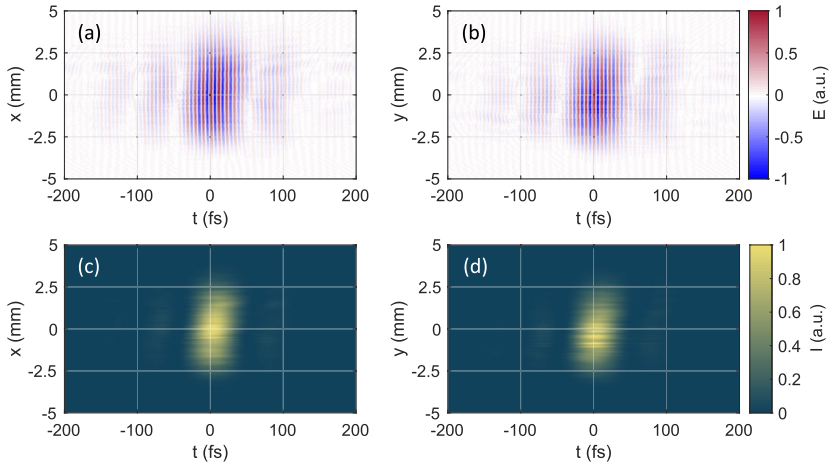

Fig. 6. Spatially resolved temporal distribution of the normalized electric field (a and b), and of the intensity (c and d) retrieved by ICE in the horizontal and vertical cross-sections, respectively.

6. Conclusion

In conclusion, we have performed for the first time to the best of our knowledge, a complete spatio-spectral characterization on few-cycle pulses around 3.2 μm central wavelength by using the spatially resolved Fourier spectroscopy. Furthermore, we combined the spatio-spectral map of the MIR pulses with their full temporal reconstruction by the TIPTOE technique and compared the retrieved spectra with the measurement results of a MOZZA spectrometer. This way, we were able to reconstruct the spatio-temporal structure of the MIR pulses and quantify the spatio-temporal couplings with high resolution. The relatively large input energy requirement of TIPTOE did not allow us to sample only a small aperture from the beam, which in general would be a more adequate way to use as a reference for the ICE retrieval. On the other hand, since the spatially resolved spectral information confirmed that the MIR pulses had a highly homogeneous spectral content over the beam cross-section, our results are still accurate. In future implementations, the accuracy of matching the temporal and spatio-spectral information can be further improved by using a less energy hungry temporal characterization method (frequency

Optics EXPRESS

resolved optical gating, dispersion scan) in combination with small sub-aperture beam sampling. This will allow for accurate spatio-temporal characterization even for pulses with significant STCs. Here we note that results of the relatively easy-to-implement ICE measurement on their own provide complete information on the spatio-spectral structure of the measured pulses. The ICE technique is also able to measure the frequency resolved wavefront of vortex pulses with orbital angular momentum, which can be utilized to generate vortex high harmonics [24].

Funding. European Regional Development Fund (GINOP-2.3.6-15-2015-00001); HORIZON EUROPE European Innovation Council (101058075 – SISHOT, 101138580 - SICEP).

Acknowledgment. The beamtime on the MIR laser of the ALPS Facility is greatly acknowledged within the framework of the 4th ELI ERIC User Call with project number ELIUPM4-111-MIR-MIRICE-RR. We also thank Balázs Bagó for programming the acquisition software for the measurements.

Disclosures. The authors declare no conflicts of interest.

Data availability. Data underlying the results presented in this paper are not publicly available at this time but may be obtained from the authors upon reasonable request.

References

1. Z. S. Heiner, L. Wang, V. Petrov, *et al.*, "Broadband vibrational sum-frequency generation spectrometer at 100 kHz in the 950-1750cm−1 spectral range utilizing a LiGaS2 optical parametric amplifier," Opt. Express **27**(11), 15289–15297 (2019).
2. B. Wolter, M. G. Pullen, M. Baudisch, *et al.*, "Strong Field Physics with Mid-IR Fields," Phys. Rev. X 5, 021034.
3. S. K. Jongkyoon Park, A. Subramani, and M. F. Ciappina, "Recent trends in high-order harmonic generation in solids," Adv. Phys.:X **7**(1), 2003244 (2022).
4. A. Baltuška, Th. Udem, M. Uiberacker, *et al.*, "Attosecond control of electronic processes by intense light fields," Nature **421**(6923), 611–615 (2003).
5. S. W. Jolly, O. Gobert, and F. Quéré, "Spatio-temporal characterization of ultrashort laser beams: a tutorial," J. Opt. **22**(10), 103501 (2020).
6. N. Thiré, R. Maksimenka, B. Kiss, *et al.*, "Highly stable, 15 W, few-cycle, 65 mrad CEP-noise mid-IR OPCPA for statistical physics," Opt. Express **26**(21), 26907–26915 (2018).
7. M. Neuhaus, H. Fuest, M. Seeger, *et al.*, "10 W CEP-stable few-cycle source at 2 µm with 100 kHz repetition rate," Opt. Express **26**(13), 16074–16085 (2018).
8. M. Mero, Z. S. Heiner, V. Petrov, *et al.*, "43 W, 1.55 µm and 12.5 W, 3.1 µm dual-beam, sub-10 cycle, 100 kHz optical parametric chirped pulse amplifier," Opt. Lett. **43**(21), 5246–5249 (2018).
9. M. F. Seeger, D. Kammerer, J. Blöchl, *et al.*, "49 W carrier-envelope-phase-stable few-cycle 2.1 µm OPCPA at 10 kHz," Opt. Express **31**(15), 24821–24834 (2023).
10. K. F. Lee, K. J. Kubarych, A. Bonvalet, *et al.*, "Characterization of mid-infrared femtosecond pulses [Invited]," J. Opt. Soc. Am. B **25**(6), A54–A62 (2008).
11. N. C. Geib, R. Hollinger, E. Haddad, *et al.*, "Discrete dispersion scan setup for measuring few-cycle laser pulses in the mid-infrared," Opt. Lett. **45**(18), 5295–5298 (2020).
12. W. Cho, S. I. Hwang, C. H. Nam, *et al.*, "Temporal characterization of femtosecond laser pulses using tunneling ionization in the UV, visible, and mid-IR ranges," Sci. Rep. **9**(1), 16067 (2019).
13. G. Pariente, V. Gallet, A. Borot, *et al.*, "Space–time characterization of ultra-intense femtosecond laser beams," Nat. Photonics **10**(8), 547 (2016).
14. M. Miranda, M. Kotur, P. Rudawski, *et al.*, "Spatiotemporal characterization of ultrashort laser pulses using spatially resolved Fourier transform spectrometry," Opt. Lett. **39**(17), 5142–5145 (2014).
15. A. Borot and F. Quéré, "Spatio-spectral metrology at focus of ultrashort lasers: a phase-retrieval approach," Opt. Express **26**(20), 26444–26461 (2018).
16. A. Jeandet, S. W. Jolly, A. Borot, *et al.*, "Survey of spatio-temporal couplings throughout high-power ultrashort lasers," Opt. Express **30**(3), 3262–3288 (2022).
17. Y. F. Chen, Z. Y. Huang, D. Wang, *et al.*, "Single-scan, dual-functional interferometer for fast spatio-temporal characterization of few-cycle pulses," Opt. Lett. **45**(18), 5081–5084 (2020).
18. J. Pan, Y. Chen, Z. Huang, *et al.*, "Self-Referencing 3D Characterization of Ultrafast Optical-Vortex Beams Using Tilted Interference TERMITES Technique," Laser Photonics Rev. **17**(4), 2370019 (2023).
19. J. Blöchl, J. Schötz, A. Maliakkal, *et al.*, "Spatiotemporal sampling of near-petahertz vortex fields," Optica **9**(7), 755–761 (2022).
20. M. Mamaikin, E. Ridente, F. Krausz, *et al.*, "Spatiotemporal electric-field characterization of synthesized light transients," Optica **11**(1), 88–93 (2024).
21. Y. Liu, S. Gholam-Mirzaei, D. Khatri, *et al.*, "Field-resolved space–time characterization of few-cycle structured light pulses," Optica **11**(6), 846–851 (2024).
22. D. N. Purschke, A. Korobenko, A. Staudte, *et al.*, "Inline-delay Fourier transform imaging spectrometer for mid-IR ultrashort pulses," Opt. Express **32**(21), 37635–37644 (2024).

Optics EXPRESS

23. ELI ERIC User portal, MIR laser source description: https://up.eli-laser.eu/laser/mir-1101562954
24. J. Qian, Y. Peng, Y. Li, *et al.*, "Femtosecond mid-IR optical vortex laser based on optical parametric chirped pulse amplification," Photonics Res. **8**(3), 421–425 (2020).